Robotica (2001) volume 19, pp. 149–161. Printed in the United Kingdom © 2001 Cambridge University Press

Contribution to the study of dynamics and dynamic control of robots interacting with dynamic environment

Miomir Vukobratovic*, †Veljko Potkonjak and Vladimir Matijevic*

(Received in Final Form: August 1, 2000)

KEYWORDS: Dynamic control; Dynamic environment; Robots control

SUMMARY

The paper discusses some practical problems of contact dynamics. Modelling the dynamics of contact tasks is carried out in a completely general way. Two dynamic systems, active robot system and passive environment system are brought into contact and the relevant dynamics are analyzed. The effects are: rigid-body contact force, elastodynamics in contact zone, friction in contact points, etc. Simultaneous stabilization of contact force and position is obtained using New Dynamic Position/Force Control. The general model is then applied to some more concrete problem and the simulation results are presented.

KEYWORDS: Dynamic control; Dynamic environment; Robots control

1. INTRODUCTION

Contact problems in robot dynamics represent a very complex field of research. They relate to different areas of theoretical and applied mechanics, electromechanics, control theory, etc. From the standpoint of mechanics one has to consider the issues of multibody dynamics, elasticity, friction and impact. Additional problems appear with the numerical approach to contact dynamics. Interaction of different effects (elasticity, friction, etc.) makes simulation experiment rather complex. On the other hand, the theory developed to support contact problems solutions in robotics can be extended thus becoming applicable to non-robotic problems. Let us concentrate on the problem of interaction between two mechanical systems.

It is well known that many robotic tasks include some kind of contact with the environment. Some of them are simple (like spot welding) but lots of them are rather complex (deburring or assembling). Control of such tasks could not be realized in the usual manner. Precise contact force realisation appeared to be of main importance for successful operation. This led to force control problems. Mathematical models describing contact dynamics offer the possibility to examine different effects relevant for position/force control. This leads to more appropriate control algorithms. The mathematical models are also used to create simulation routines. The next important role of contact dynamic analysis lies in the possibility to design robots or some robot tools so as to support specific requirements of contact tasks.

The fact that many robot tasks include the contact of the end-effector and the robot environment led to the first research on contact dynamics.[1,2] Robot environment was considered in the form of a geometric constraint. Stationary and non-stationary cases were considered. The constraints imposed to the end-effector resulted in reaction forces. Dynamic models were derived for arbitrary constraints (restricting one to six degrees of freedom). All robot elements were considered rigid. The derived models enabled solution of motion along with computation of contact forces. Friction between robot and environment was included. Some practical examples considered were the writing and assembly task.

The next extension in this research was to introduce the constraints upon the motion of the end-effector, and thus, consider elastic joint robots in contact tasks. Several approaches to simultaneous force and position control in constrained robot systems with joint flexibility have been proposed in the literature.[3–7]

Further, elastic effects can be expressed with the robot base. If connections of the robot arm and its base were considered deformable or if the robot for instance was placed on a platform with pneumatic wheels, then oscillations would appear. These effects can be included in the existing models of rigid system, by adding some kind of passive DOFs. Similar problems may appear on the environment side. If the object that should be grasped or processed in some other way was connected to its base by means of deformable connections, then oscillations would arise. The dynamic model of environment is then needed.

Most research effort in contact dynamics were made with the aim of creating the adequate control strategies for contact task control. Different approaches to the problem solution of contact tasks control can be distinguished. Among these, two approaches should be recognized: hybrid position/force control[8–11] and impedance control.[12,13] Hybrid control consists of two parallel feedback loops (Fig. A.1), the upper one for the position, and the lower one for the force feedback loop. Each of these loops uses separate sensor systems. Impedance control represents a strategy for constrained motion rather than a concrete control scheme. Environment was modeled by appropriate impedance. Thus, dynamics took place, but with the restriction to linear model. The complete dynamics of environment, including

* Robotics Department, Mihajlo Pupin Institute, P.O. Box 15, 11000 Belgrade (Yugoslavia)
† Electrical Engineering Faculty, Bulevar Revolucije 73, 11000 Belgrade Yugoslavia

https://doi.org/10.1017/S0263574700003064 Published online by Cambridge University Press

nonlinear effects and non-holonomic constraints is the topic of new dynamic control of robots interacting with dynamic environment.[14–16]

The purpose of this work is to derive the general dynamic contact model and to apply it to assembling contact task.

2. MATHEMATIC FORMULATION OF RIGID-BODY CONTACT

The discussion on contact dynamics starts with two rigid-body systems. The systems are assumed to be in the form of active chains (Fig. 1). The intention is to make the discussion general and treat the two systems equally. However, we find that for easier understanding it is useful to name the systems. Let one of them be called the *working system* (or *robot*) and the other the *complex dynamic environment* (or simply *environment*). The discussion on contact of two mechanical systems need not be connected to robotics. However, we are mainly interested in robotic implementation. Thus, by the term working system we mainly understand some kind of a manipulator (a simple manipulation system or a robot). What is meant by environment? It is a dynamic system with active or passive degrees of freedom (DOFs) working in cooperation with a robot or assisting it. In practical problems, it can represent a rotating or coordinate table, some more complex positioner, conveyor, transport cart, CNC machine (e.g. lathe), another robot, etc. The names introduced for the two systems do not restrict the possibility of applying the following discussion to other sort of mechanical systems.

At the beginning we consider the two geometrically and dynamically uncoupled chains (Fig. 1a) and write their dynamic models. Let the working system (robot) has n_r DOFs (index "*r*" will be used for all working system variables). The environment has n_e DOFs (index "*e*" will be used for all environment variables). If chain (*r*) (see Fig. 1a) is a robot, then it usually has $n_r = 6$ DOFs. However, for the environment chain (*e*) one can hardly predict the number of DOFs. If a rotating table is in question, then it has $n_e = 1$ DOF. For an *X*-*Y* table, it would be $n_e = 2$, and if another robot is in question then it might be $n_e = 6$.

The internal position vectors are $q_r = (q_{r1}, \ldots, q_{rn_r})$ and $q_e = (q_{e1}, \ldots, q_{en_e})$. They define the motion of joints. The position of the entire system may be expressed by the united vector of dimension $n = n_r + n_e$:

$$q = \begin{bmatrix} q_e \\ q_r \end{bmatrix}. \tag{1}$$

The dynamics of the two decoupled chains can be described by means of model:

$$H_e(q_e)\ddot{q}_e + h_e(q_e, \dot{q}_e) = \tau_e \tag{2}$$

$$H_r(q_r)\ddot{q}_r + h_r(q_r, \dot{q}_r) = \tau_r, \tag{3}$$

where H_e and H_r are inertial matrices, and h_e, h_r take care of gravity, Coriolis' forces and other position-dependent and velocity dependent forces if they are present, τ_e and τ_r are joint torque vectors. There are reasons why the environment model is placed first and the robot model later. This will be explained when introducing the set of functional coordinates.

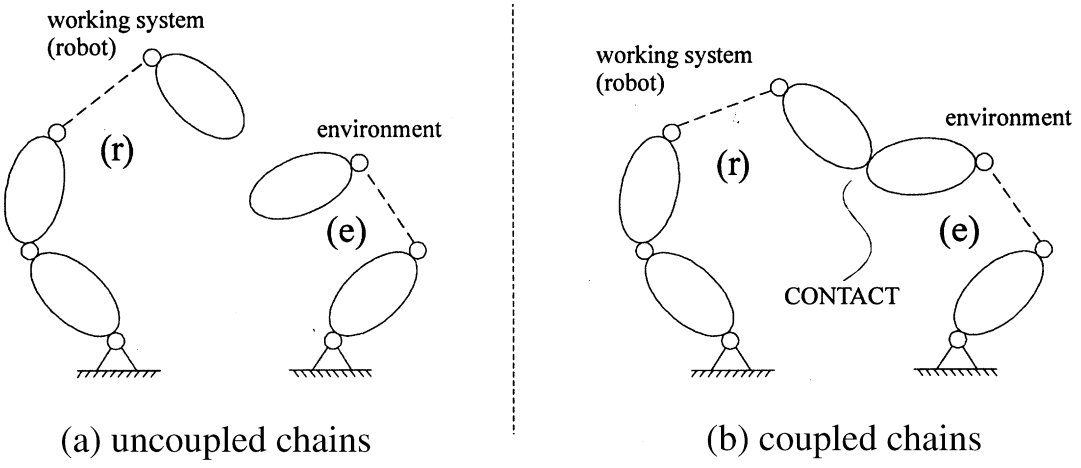
For each chain, one may introduce a set of functional coordinates describing the position in the most proper way for a particular problem. Let $s_e = (s_{e1}, \ldots, s_{en_e})$ and $s_r = (s_{r1}, \ldots, s_{rn_r})$ be the functional coordinates for the two chains. Relation between coordinates q and s represents the kinematic model. For the environment, s-coordinates are defined as absolute. This means that these coordinates describe the environment position with respect to the immobile (absolute) frame. Very often set s_e, coincides with q_e since it may be impossible to find a more suitable set of coordinates. In a general case,

$$s_e = s_e(q_e) \tag{4}$$

represents a nonlinear function. The operation of robot usually understands some prescribed relation with the environment. The relation includes kinematic behavior and sometimes dynamic effects as well. Hence, it is suitable to define the s-coordinates of a robot as relative. They describe the position of a robot (its end-effector) with respect to the environment (i.e., to a frame fixed to the terminal link of the environment chain (e)). Accordingly, the transformation of coordinates has the form:

$$s_r = s_r(q_e, q_r) \tag{5}$$

The set of functional coordinates of the entire system is:



(a) uncoupled chains (b) coupled chains

Fig. 1. Two kinematic chains: (a) in free motion, and (b) in contact motion.

https://doi.org/10.1017/S0263574700003064 Published online by Cambridge University Press

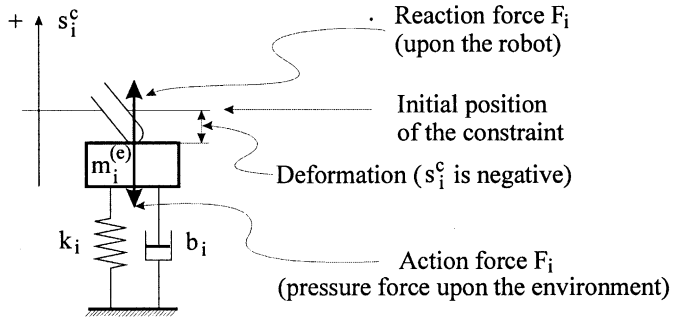


Fig. 2. Deformation coordinates and reaction forces in environment model.

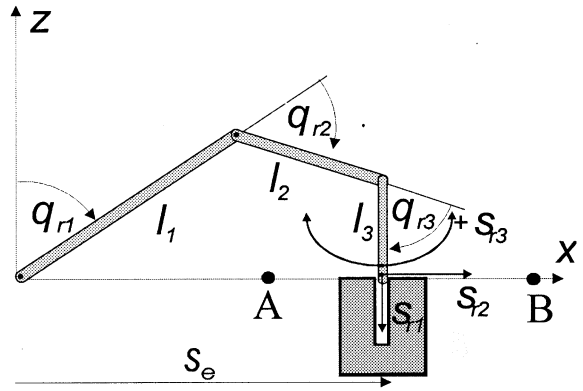


Fig. 3. Peg-in-hole task. The task is being solved by a three-joint robot.

Table I. Parameters of the robot mechanism.

J	$l_j[m]$	$m_{rj}[kg]$	J_{rj}
1	1.	20.	$J_{rj}=\frac{1}{12}m_{rj}l_j^2$
2	0.6	10.	
3	0.4	5.	

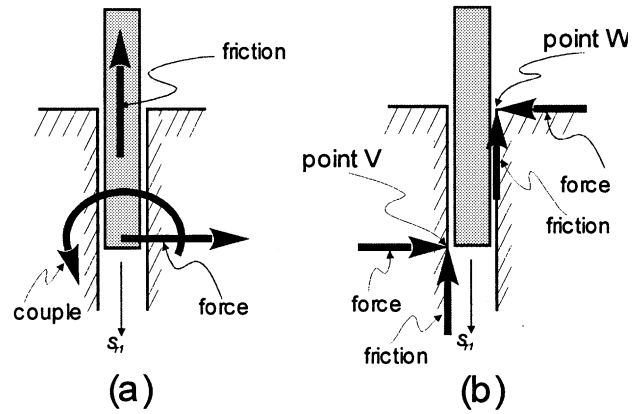


Fig. 4. Two approaches to the contact action/reaction: (a) a force and a couple express the influence between the robot and the cart, (b) two forces are used to express the influence.

$$s=\begin{bmatrix} s_e \\ s_r \end{bmatrix}. \tag{6}$$

Let us now discuss the contact between the two chains (Fig. 1b). We note that the relative coordinates s_r are defined so as to support the prescribed task. Hence, it is justified to assume that contact can be expressed by means of zero-values of some of these coordinates. If we suppose that the contact restricts m DOFs, then m coordinates from set s_r reduce to zero. Now it is convenient to separate vector s into two subvectors but in a way different from Eq. (6). Let the set s^c contain the coordinates constrained by the contact (all from s_r) and have dimension m ($m \le n_r$). The remaining coordinates from s_r ($n_r - m$ of them) are free. If s^f is the set of free coordinates of the entire system, then it includes the complete vector s_e, plus $n_r - m$ elements of vector s_r. Dimension of s^f is $n_e + n_r - m$. The new separation is:

$$s=\begin{bmatrix} s^f \\ s^c \end{bmatrix} \tag{7}$$

The constraint (contact) is now expressed as:

$$s^c = s^c(q_e, q_r) = 0 \tag{8}$$

This means that rigid-body contact is considered and modeled by applying geometric constraints. From the dynamic point of view, contact causes a reaction force (contact force). The number of force components equals the number of restricted DOFs. In this case model (2), (3) should include the contact force F of dimension m:

$$H_e(q_e)\ddot{q}_e + h_e(q_e, \dot{q}_e) = \tau_e + J_e^{cT}(q_e, q_r)F \tag{9}$$

$$H_r(q_r)\ddot{q}_r + h_r(q_r, \dot{q}_r) = \tau_e + J_r^{cT}(q_e, q_r)F \tag{10}$$

where J_e^c and J_r^c are Jacobian matrices: $J_e^c = \partial s^c/\partial q_e$ and $J_r^c = \partial s^c/\partial q_r$, of dimensions $m \times n_e$ and $m \times n_r$, respectively.

Coordinates q_e and q_r appearing in (9) and (10) are not independent due to constraint (8). Accordingly, models (9) and (10) along with condition (8) describe the dynamics of the entire system. It is more convenient if the constraint relation is written in a differential form. The first derivative of s^c gives:

$$\dot{s}^c = \frac{\partial s^c}{\partial q_e}\dot{q}_e + \frac{\partial s^c}{\partial q_r}\dot{q}_r = J_e^c\dot{q}_e + J_r^c\dot{q}_r, \tag{11}$$

and the second derivative:

$$\ddot{s}^c = J_e^c\ddot{q}_e + J_r^c\ddot{q}_r + A^c, \tag{12}$$

where matrices J_e^c and J_r^c are the same ones introduced in Eqs. (9) and (10) and the adjoint vector is

$$A^c = (\partial^2 s^c)/(\partial q_e)^2\dot{q}_e^2 + (\partial^2 s^c)/(\partial q_e \partial q_r)\dot{q}_e\dot{q}_r + (\partial^2 s^c)/(\partial q_r \partial q_e)\dot{q}_r\dot{q}_e + (\partial^2 s^c)/(\partial q_r)^2\dot{q}_r^2$$

The constraint (8), if written in second order differential form, becomes

$$\ddot{s}^c = J_e^c\ddot{q}_e + J_r^c\ddot{q}_r + A^c = 0. \tag{13}$$

https://doi.org/10.1017/S0263574700003064 Published online by Cambridge University Press

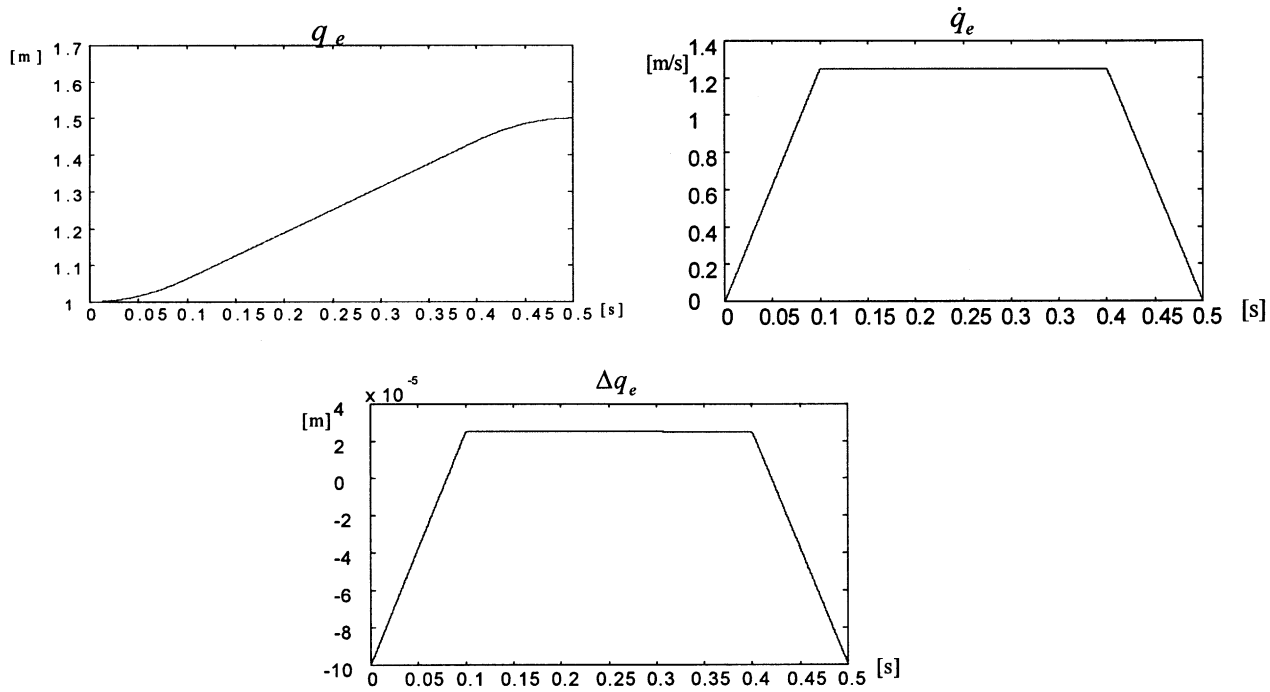


Fig. 5. Simulation; rigid-body contact and classical hybrid control: time histories of cart motion (q_e), its tracking error (q_e), and velocity ($\dot{q}_e$).

Dynamics is now described by model (9), (10) along with relation (13). This is a set of $n_e + n_r + m$ scalar equations that can be solved for the same number of scalar unknowns: n_e components of acceleration $\ddot{q}_e$, n_r components of acceleration $\ddot{q}_r$, and m components of force F. Thus, simulation is possible.

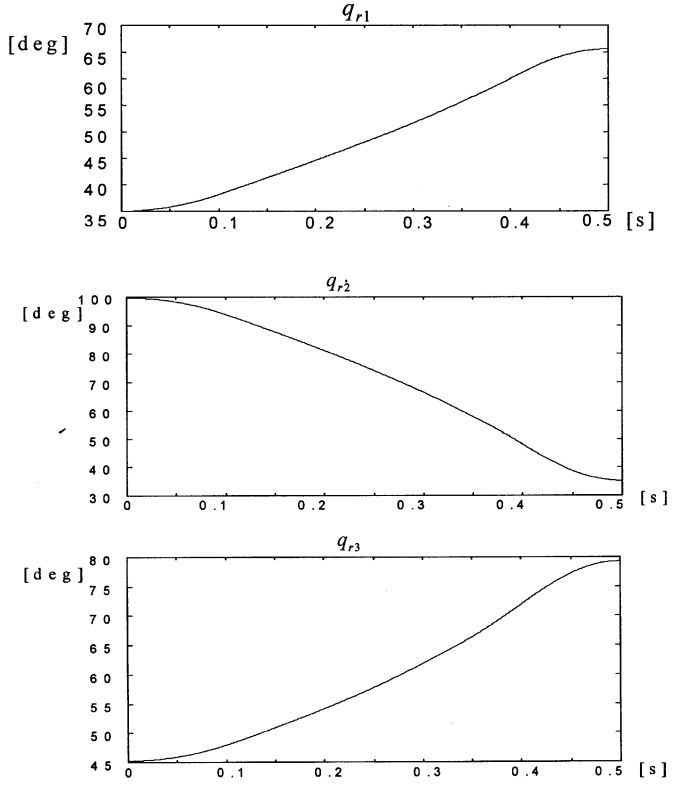


Fig. 6. Simulation; rigid-body contact and classical hybrid control: time histories of robot joint coordinates q_{r1}, q_{r2} and q_{r3}.

3. MODELING FRICTION EFFECTS

With the approach used, the contact influenced a subset of functional coordinates: s^c was kept zero by means of the reaction force F acting in the direction of coordinates s^c. The resting coordinates (subset s^f) were free and there was no resistance in these directions. However, in real situation some kind of friction force always exists. Friction appears between two bodies in contact. We shall consider friction force and include it in the dynamic model. Friction appears between two bodies into the contact. Let us separate $s^f = (s_e, s_r^f)$ where s_r^f contains n_r–m free coordinates. Friction force can be expressed in the form:

$$F_f = -|F_f|\,\nu_o \tag{14}$$

where F_f is (n_r–m) component friction vector, $|F_f|$ is its absolute value, and ν_o is (n_r–m)-component vector defining the direction of relative velocity (unit vector). The absolute value $|F_f|$ depends on the contact force, quality of the surface and on the relative velocity. With a more complex contact it may depend on some other parameters, too (geometric parameters like area of contact). In the majority of practical problems it is justified to assume $|F_f| = \mu|F|$ where μ is constant coefficient. More exact modelling should introduce the dependence on velocity.

Direction on vector ν_o depends on relative velocity $\dot{s}_r^f$ which can be expressed in the Jacobian form:

$$\dot{s}_r^f = J_{rr}^f(q_e, q_r)\dot{q}_r + J_{re}^e(q_e, q_r)\dot{q}_e, \tag{15}$$

where $J_{rr}^r = \partial s_r^f / \partial q_r$ and $J_{re}^f = \partial s_r^f / \partial q_e$.

The discussion on friction force showed that it might be expressed generally as:

$$F_f = F_f(F, q_e, q_r, \dot{q}_e, \dot{q}_r) \tag{16}$$

This form of friction force now enters the mathematical model of system dynamics. Equations (9) and (10) become:

https://doi.org/10.1017/S0263574700003064 Published online by Cambridge University Press

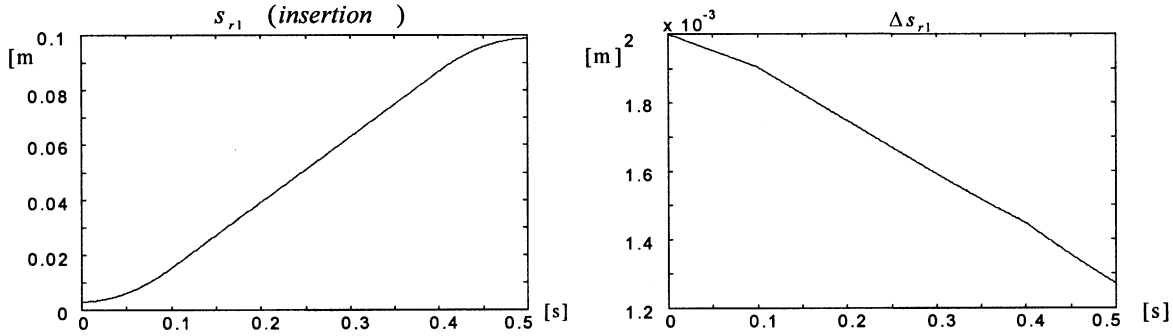


Fig. 7. Simulation; rigid-body contact and classical hybrid control: insertion coordinate s_{r1}, and its tracking error Δs_{r1}.

$$H_e(q_e)\ddot{q}_e + h_e(q_e, \dot{q}_e) = \tau_e + J_e^{cT}(q_e, q_r)F + J_{re}^{fT}(q_e, q_r)F_{fr} \quad (17)$$

$$H_r(q_r)\ddot{q}_r + h_r(q_r, \dot{q}_r) = \tau_r + J_r^{cT}(q_e, q_r)F + J_{rr}^{fT}(q_e, q_r)F_{fr} \quad (18)$$

With the friction expressed by (16), dynamic model (17), (18) along with relation (13) (expressing the contact) can be solved for $n_e + n_r + m$ scalar unknowns: n_e-component acceleration $\ddot{q}_e$, n_r-component acceleration $\ddot{q}_r$, and m-component force F. Thus, simulation is possible.

We remember that the above discussion holds while the tip slides over the surface. When it stops, friction force becomes unknown. This situation was called jamming. The stopping may be expressed by:

$$\dot{s}_r^f = J_{rr}^f(q_e, q_r)\dot{q}_r + J_{re}^f(q_e, q_r)\dot{q}_e = 0, \quad (19)$$

or in the second order form:

$$\ddot{s}_r^f = J_{rr}^f(q_e, q_r)\ddot{q}_r + J_{re}^f(q_e, q_r)\ddot{q}_e + A_r^f = 0. \quad (20)$$

Dynamic model (17), (18) along with relations (13) (expressing the contact) and (19) (expressing jamming) consists of $n_e + n_r + m + n_r - m$ scalar equations that can be solved for the same number of unknowns: $\ddot{q}_e$ (n_e components); $\ddot{q}_r$ (n_r components), F (m component), and F_{fr} ($n_r - m$ components). Jamming ends and the tip starts to move when the magnitude of the friction force reaches the value μF.

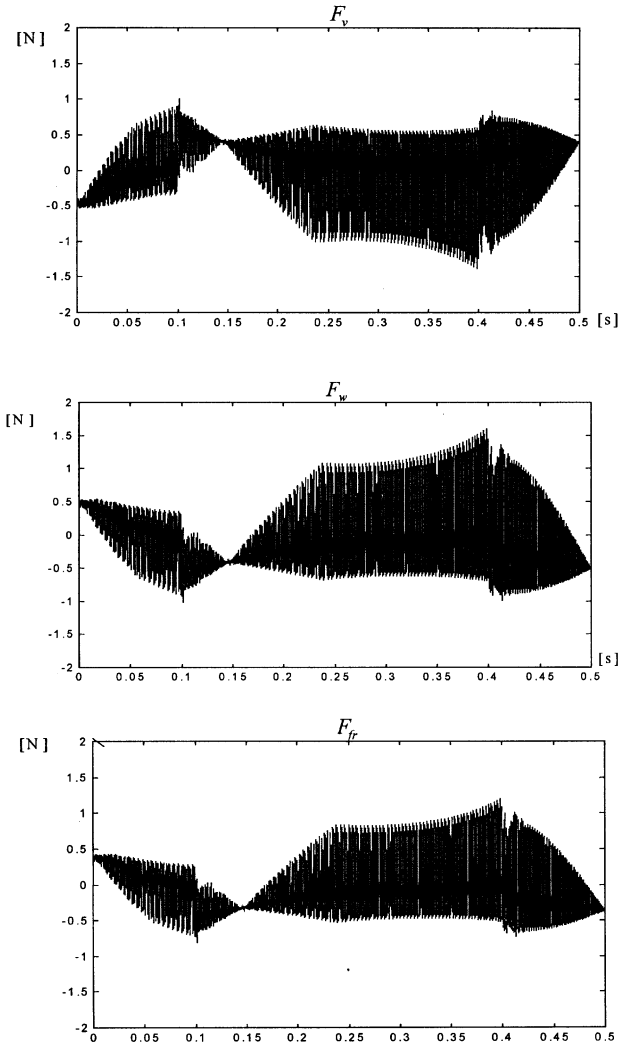


Fig. 8. Simulation; rigid-body contact and classical hybrid control: contact forces F_V and F_W, and the total friction force F_{fr}.

4. INTRODUCING A DYNAMIC ENVIRONMENT

In the previous text, it was assumed that both chains consisted of rigid bodies. We now introduce elastic effects in the contact zone. In the previous text rigid constraint was defined by zero values of some functional coordinates: $s^c = 0$, where subvector s^c contained m constrained coordinates. The remaining 6-m coordinates were free and formed subvector s^f. If the environment is not rigid but deformable coordinates s^c need not be zero any more. Deviation from zero represents elastic deformation. This means that these coordinates (s^c) are not geometrically

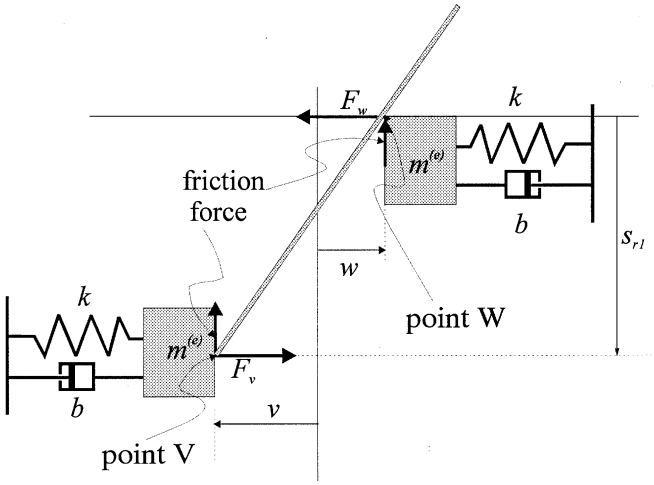


Fig. 9. Elastodynamic contact. Deflections in the two contact points are introduced. Each deflection is characterized by an equivalent mass, stiffness and damping.

https://doi.org/10.1017/S0263574700003064 Published online by Cambridge University Press

constrained. Theoretically they may take any value. However, relatively high stiffness keeps the magnitude of coordinates small. Although all *s*-coordinates are now free, we still keep separation of vector *s* into s^f and s^c. Subvector s^c consists of deformation coordinates while s^f involves those which are "really free".

We will adopt that robot is absolutely rigid, or that the elasticity of the robot is much smaller than that of the environment, which is a reasonable assumption for most of the problems. Environment will be modeled as elastodynamic environment (Fig. 2).

If the environment is modeled as shown in Fig. 2, the Newton's law gives the expression for the force:

$$F_i = -m_i^{(e)} \ddot{s}_i^c - k_i s_i^c - b_i \dot{s}_i^c, \tag{21}$$

where $m_i^{(e)}$ is the equivalent mass, and k_i, b_i are the stiffness and damping along the direction of the coordinate s_i^c. For all directions from the set s^c (m components) one may write a matrix expression

$$F = -m^{(e)} \ddot{s}^c - k s^c - b \dot{s}^c, \tag{22}$$

where $m^{(e)} = diag[m_i^{(e)}]$ is the m-dimensional inertial matrix, $k = diag[k_i]$ is the stiffness matrix, and $b = diag[b_i]$ is the damping matrix.

Complete model of the dynamics of the contact task is now expressed by kinematics equations (12), (15), relation (16) which models friction force and dynamics equations (17–18). These equations can be solved.

5. CASE STUDY

We consider an in-process operation. A robot has to insert a peg into a hole. The object with a hole is placed on a transport cart. Scheme of the task is given in Fig. 3. In this scheme, the peg is shown as being a part of the robot terminal link. The cart and the object with the hole are considered as one body and simply called the cart.

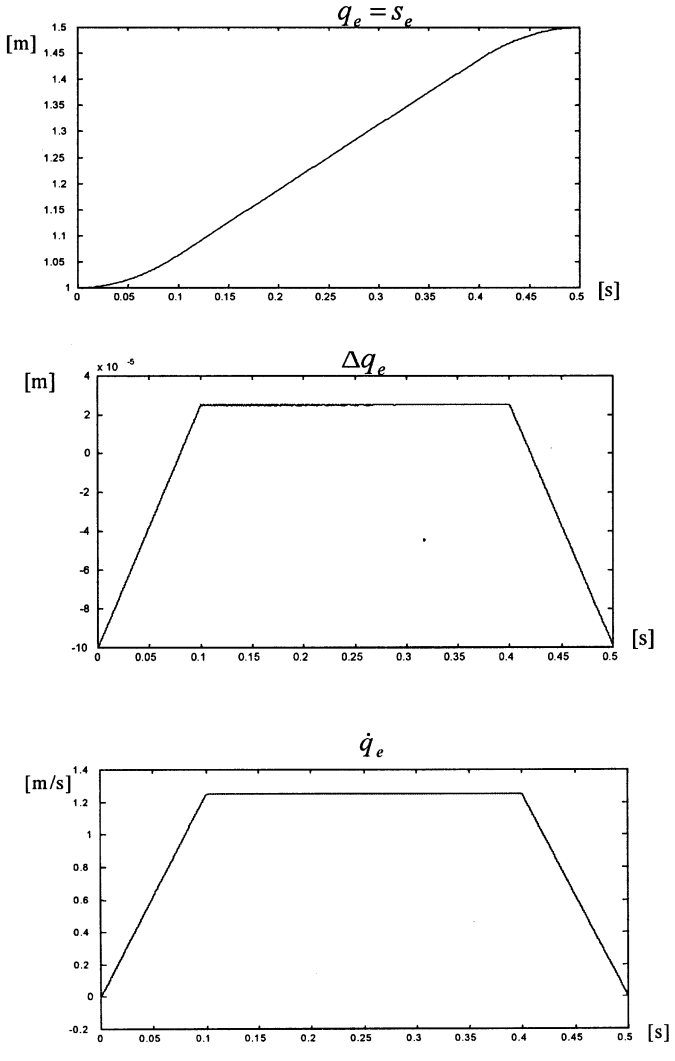


Fig. 10. Simulation; elastodynamic contact and classical hybrid control: time histories of cart motion (Δq_e), its tracking error (q_e), and velocity ($\dot{q}_e$).

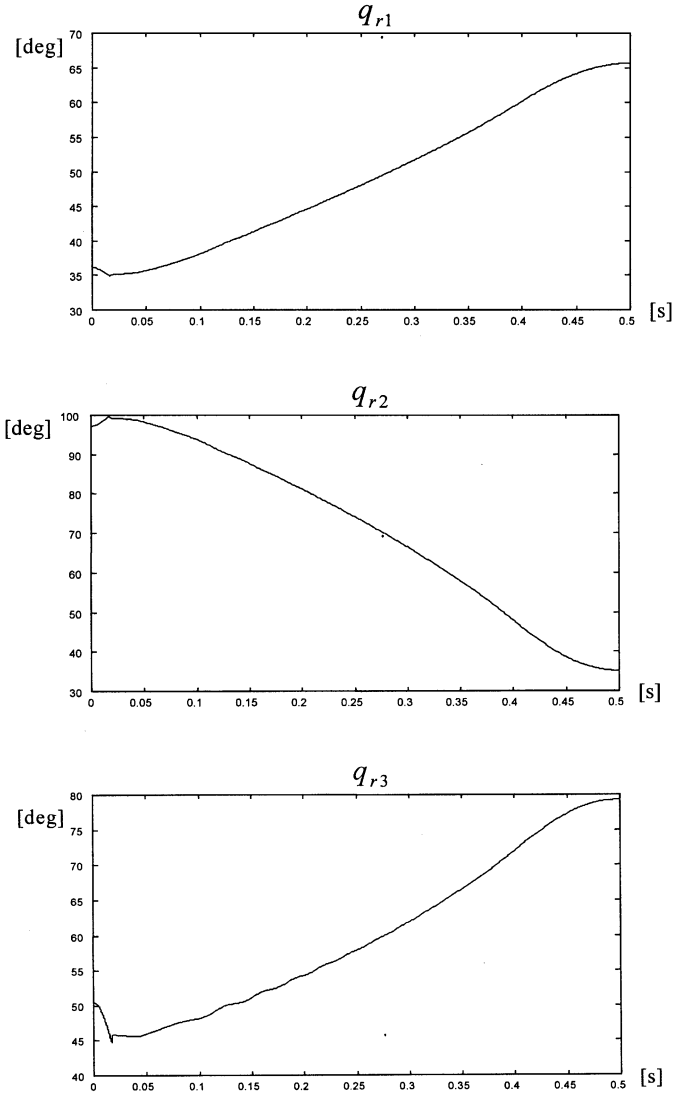


Fig. 11. Simulation; elastodynamic contact and classical hybrid control: time histories of robot joint coordinates q_{r1}, q_{r2} and q_{r3}.

https://doi.org/10.1017/S0263574700003064 Published online by Cambridge University Press

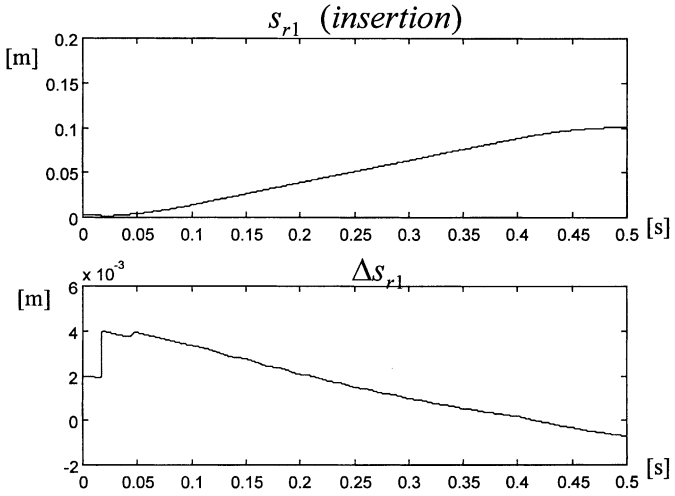


Fig. 12. Simulation; elastodynamic contact and classical hybrid control: insertion coordinate s_{r1}, and its tracking error Δs_{r1}.

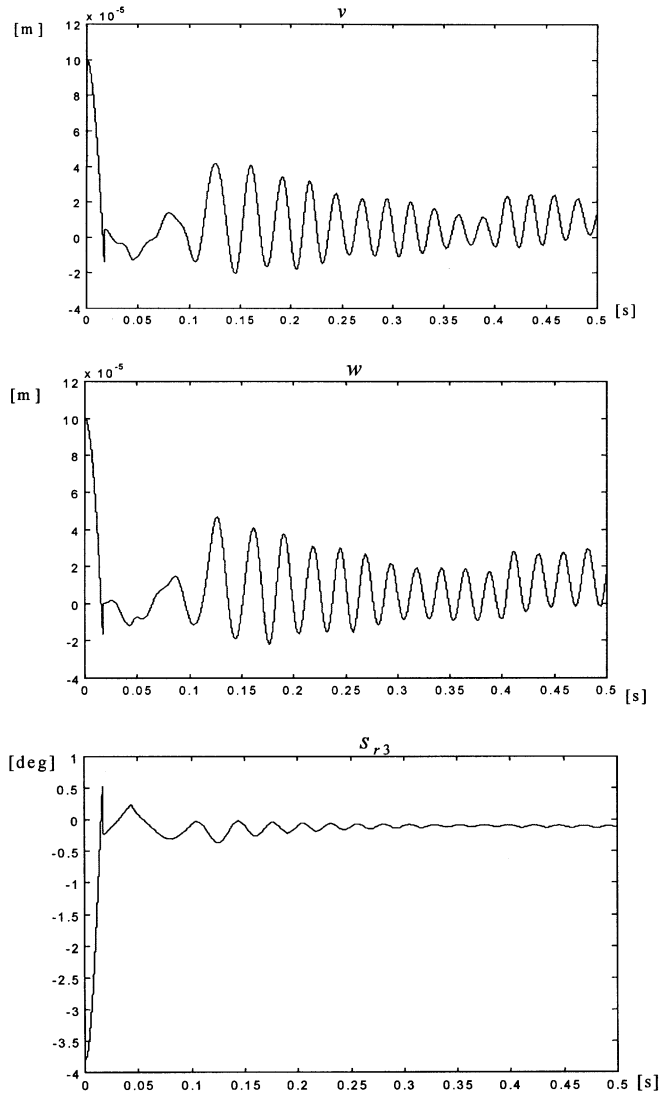


Fig. 13. Simulation; elastodynamic contact and classical hybrid control: deflections in contact points, *v* and *w*, and angular deviation of the peg.

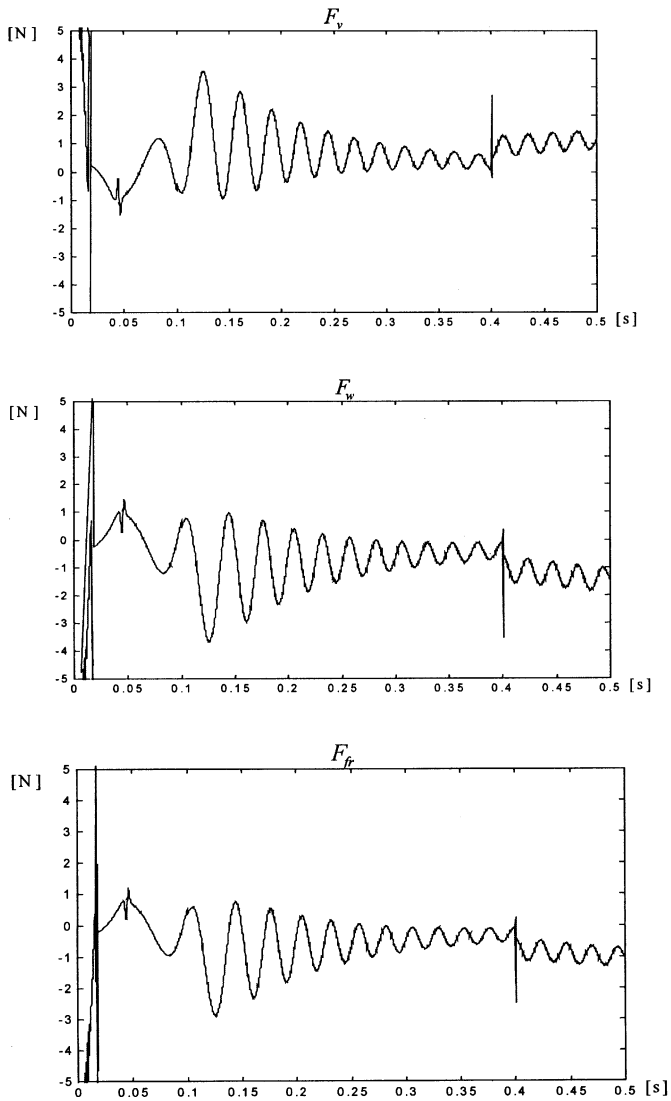


Fig. 14. Simulation; elastodynamic contact and classical hybrid control: contact forces f_v and f_w, and total friction force f_{fr}.

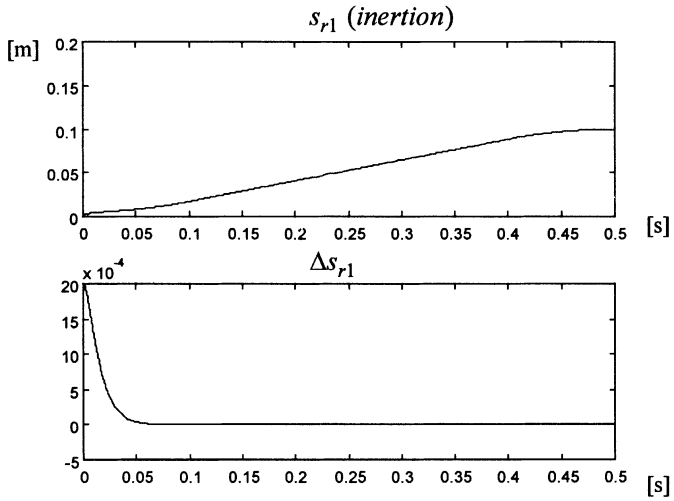


Fig. 15. Simulation; elastodynamic contact and dynamic position control: insertion coordinate s_{r1}, and its tracking error Δs_{r1}.

https://doi.org/10.1017/S0263574700003064 Published online by Cambridge University Press

The robot has three DOFs. The data about its mechanism (geometry and inertial properties) are given in Table I. Each joint is actuated by a DC motor. It is adopted that motors are equal with the following parameters: $C_M = 0.0575$N/A, $C_E = 0.0575$V/(rad/s), $R = 0.175\Omega$, $B_C = 1.432 \cdot 10^{-4}$Nm/(rad/s), and $I = 7.9 \cdot 10^{-4} kgm^2$. Reduction ratio is $N = 50$.

The cart represents the environment. Its mass is $m_e = 5$ kg. It is driven by a DC motor which is equal to those used for robot joints.

Let us explain the task. The cart moves horizontally from position A ($x_A = 1m$) to position B ($x_B = 1.5m$). The motion lasts 0.5*s*, and is performed with trapezoidal velocity profile (acceleration and deceleration take 20% of the motion time each). The robot follows the motion of the cart and at the same time inserts its terminal link (the peg) into the hole. Insertion of 0.1*m* is performed in 0.5*s*, with trapezoidal velocity profile (acceleration/deceleration time is 20%). During insertion, friction occurs between the peg and the hole. The friction coefficient is $\mu = 0.4$. It is clear that the insertion requires vertical direction of the peg (terminal link). Besides, it is desired to perform insertion with contact force equal zero.

Now, we define the position coordinates. Fro the cart, the functional *s*-coordinate coincides with the *q*-coordinate and both coincide with *x*: $s_e = q_e = x$. For the robot, the joint coordinates are: q_{r1}, q_{r2} and q_{r3}. Functional coordinates are chosen so as to define the relative position with respect to the cart. The origin of the frame is placed at the entrance of the hole. Two coordinates will define the position of the tip with respect to the origin, and the third coordinate will define the angular orientation of the terminal link. The choice is made as follows: s_{r1} represents the insertion, S_{r2} defines the horizontal distance of the tip (measured from the hole entrance), and finally, s_{r3} represents the angular deviation of terminal link from the vertical direction oriented downwardly. The complete vector *s* includes one-component vector s_e and three-component vector s_r: $s = (s_e, s_{r1}, s_{r2}, s_{r3})$. Now, one should make the new separation of vector *s* to free and constrained coordinates. Looking to the task shown in Figure 3, one can find that the cart motion and

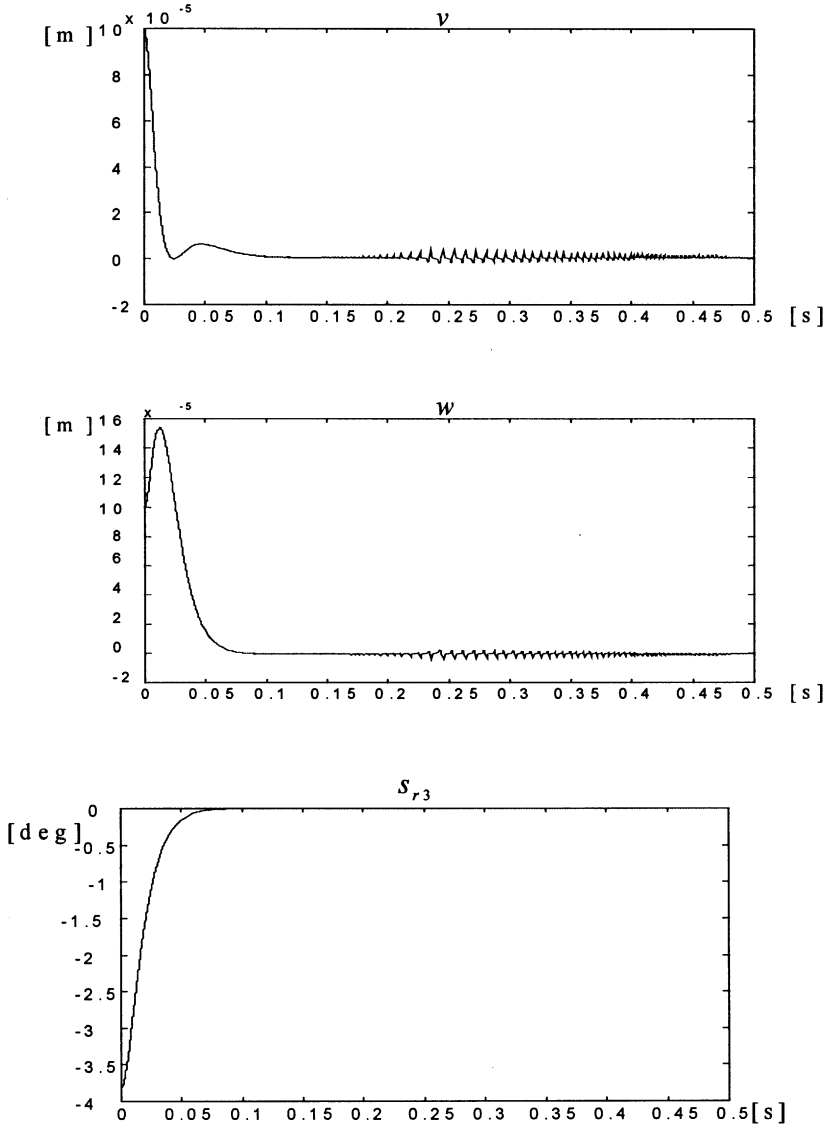


Fig. 16. Simulation; elastodynamic contact and dynamic position control: deflections in contact points, *v* and *w*, and angular deviation of the peg.

https://doi.org/10.1017/S0263574700003064 Published online by Cambridge University Press

the peg insertion represent the free coordinates: s^f (s_e, s_{r1}). The contact between the peg and the hole constrains the lateral motion and the angular motion of the peg, and thus: $s^c = (s_{r2}, s_{r3})$.

We shall discuss two cases, the rigid-body contact and the elastodynamic contact. In any case, the cart is not engaged in controlling the contact. It is forced to track the referent motion by applying the PID regulator. For the robot, we are going to try two kinds of control, conventional hybrid position-force control and dynamic position control. The concept of hybrid position/force control and dynamic control is explained in the Appendix.

5.1 The rigid-body contact

The rigid-body contact is discussed first. It is expressed by the requirement: $s^c = 0$, that is, $s_{r2} = 0$ and $s_{r3} = 0$. For controlling the robot, the conventional hybrid control law (A.2) is applied. Gains for the hybrid control law are

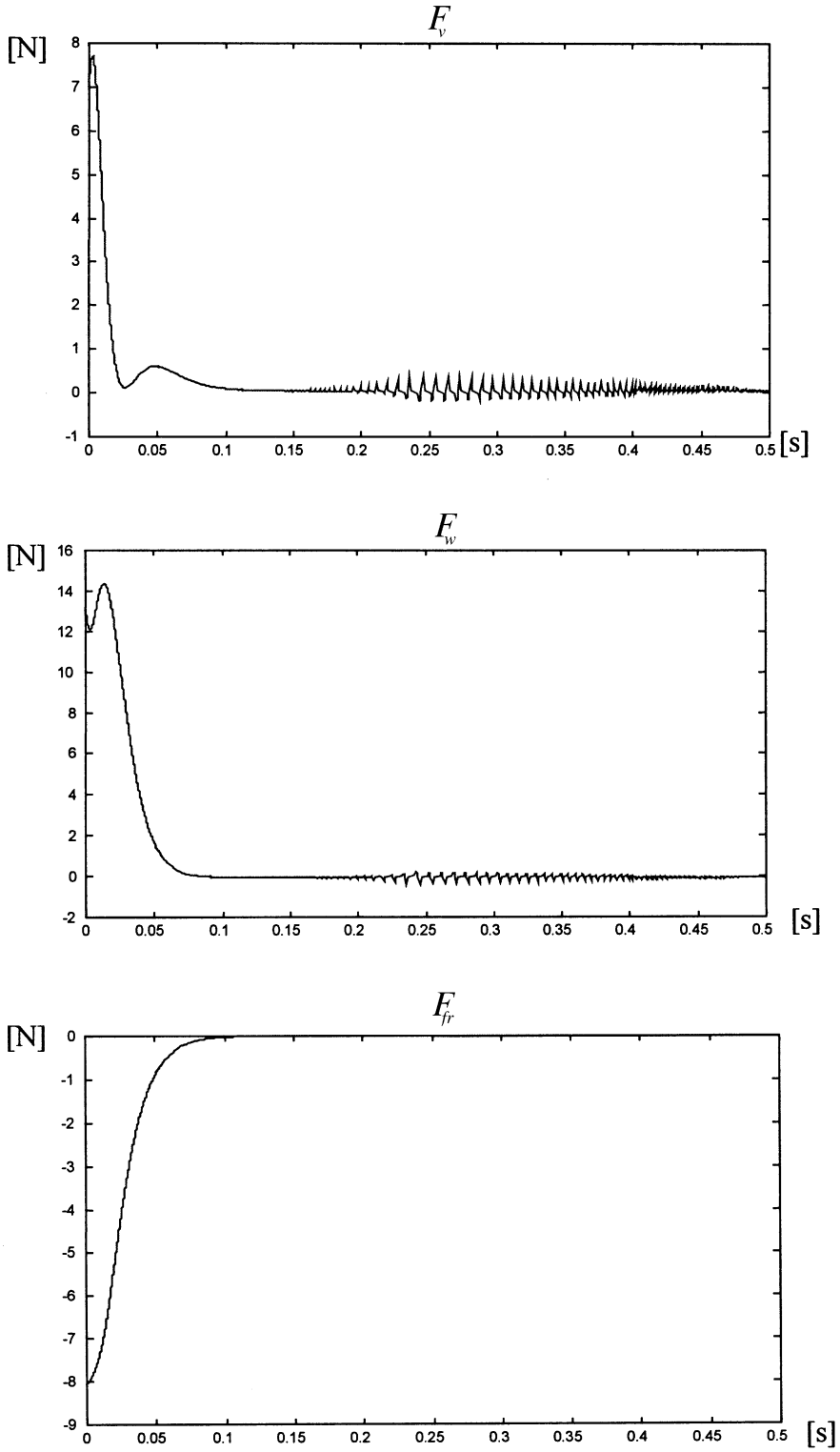


Fig. 17. Simulation; elastodynamic contact and dynamic position control: contact forces F_V and F_W, and total friction force F_{fr}.

https://doi.org/10.1017/S0263574700003064 Published online by Cambridge University Press

$K_p = 50000 \cdot I_3$; $K_v = 100000 \cdot I_3$; $K_{Fp} = 15000 \cdot I_3$; $K_{Fi} = 500 \cdot I_3$; where $I_3 = \begin{bmatrix} 1 & 0 & 0 \\ 0 & 1 & 0 \\ 0 & 0 & 1 \end{bmatrix}$. Selection matrix is $S = \begin{bmatrix} 1 & 0 & 0 \\ 0 & 1 & 0 \\ 0 & 0 & 0 \end{bmatrix}$. The cart is controlled by the PID controller with environment gains $K_{pe} = 1000$; $K_{ve} = 50000$; $K_{ie} = 100$.

The theory explained in the previous text allows to simulate the system behavior. Strictly speaking, there must exist an approaching phase, then an impact phase, and after that the "regular" insertion starts. We start presentation of the results from the moment when the impact is finished. At that instant the peg tip is inserted into the hole by 3 *mm*. So, $s_{r1}(0) = 0.003m$ represents the initial position. However, reference motion understands the insertion of 5*mm* in that instant. This means $s^*_{r1}(0) = 0.005$ and, thus, the initial error is $\Delta s_{r1}(0) = s^*_{r1} - s_{r1} = 0.002m$. Notation * indicates the reference values.

Simulation understands the calculation of the cart and robot motion as well as the calculation of contact force. Motion is described by means of internal *q*-coordinates: q_e for the cart and q_{r1}, q_{r2} and q_{r3} for the robot; or in terms of functional *s*-coordinates: s_e for the cart and s_{r1} for the robot (note that $s_{r2} = 0$ and $s_{r3} = 0$). The analysis of forces and their presentation requires some additional explanation. Contact force appears along the direction of each constrained coordinate. Hence, in the example, the contact action (or reaction) has two components, a force along the lateral direction s_{r2} and a couple along the angular direction s_{r3} (see Fig. 4a). When the peg-in-hole task is considered, it might be more convenient and more close to application if contact was considered in terms of the two forces as shown in Fig. 4b. The number of unknowns does not change since two forces replace a force and a couple. This approach will be even more beneficial when we discuss the elastodynamic contact. Regardless of the representation of contact, the friction force is introduced acting in the direction opposite to the free coordinate s_{r1} (Fig. 4a, b).

Figures 5–8 present the simulation results. Figure 5 shows the motion of the cart. Time histories of coordinatre q_e, tracking error Δq_e, and velocity q_e, are given. From these figures we can see that the cart is following the prescribed trajectory (trapezoidal velocity profile). Figure 6 shows the robot motion in terms of its internal coordinates q_{r1}, q_{r2} and q_{r3}. Figure 7 shows the insertion. Time histories of the relative coordinate s_{r1} and tracking error Δs_{r1} are presented. Figure 8 shows the contact forces F_v and F_w in points V and W, and the total friction force F_{fr}.

5.2 The elastodynamic contact

Now, we introduce elasticity in the contact zone. It is assumed that the peg is infinitely rigid, and thus, deformation appears on the cart side only. In the rigid-body consideration, the insertion, being a two-component contact, was described by zero values of the two coordinates, s_{r2} and s_{r3}. When deformation is introduced, this does not hold. Theoretically, the two coordinates may take any value, but the strong environment elastic forces will keep these values small. Thus, lateral and angular deviations of the peg, although small, should be taken into account. However, we decided to express the two-component contact in terms of the two contact points (points V and W in Fig. 4b). In the case of contact with deformation, there appears an elastic deflection in each contact point. So, instead of deviations s_{r2} and s_{r3}, we introduce deflections *v* and *w*, as shown in Figure 9. Each deflection is characterized by an equivalent mass $m^{(e)}$, stiffness *k*, and damping coefficient *b*. This means that one-stage deformation model is used. For simulation we adopt: $m^{(e)} = 1kg$, $k = 10^5 N/m$, and $b = 1N/(m/s)$.

When starting simulation, we adopted some initial position error. In the consideration of rigid-body contact, the error $\Delta s_{r1}(0) = 0.002$ m in the direction of insertion was adopted. In the case of elastodynamic contact, we keep this and add a new initial error that follows from the deformation of the hole: angular deviation $s_{r3}(0) = -3.81$deg follows from deflections $v(0) = 0.1mm$ and $w(0) = 0.1mm$.

For controlling the robot, classical hybrid control law (A.2) is applied with the same gains as in simulation with geometrical environment.

Figure 10–14 present the simulation results. Figure 10 shows the motion of the cart. Time histories of coordinate q_e, tracking error Δq_e, and velocity $\dot{q}_e$, are given. Figure 11 shows the robot motion in terms of its internal coordinates q_{r1}, q_{r2} and q_{r3}. Figure 12 shows the insertion. Time histories of the relative coordinate s_{r1} and tracking error Δs_{r1} are presented. Figure 13 shows the deformation. Deflections *v* and *w* are shown as well as the angular deviation of the peg (s_{r3}) which is the consequence of these two deviations. Figure 14 shows the contact forces F_v and F_w, and the total friction force F_{fr}.

Simulation of elastodynamic contact is repeated, but with the dynamic position control (A.8) applied to the robot (replacing the hybrid law). Vector function *P* from the dynamic position control law (A.8) was defined as $P = K_p \Delta\dot{q} + K_v \Delta\dot{q}$, where the gains are $K_p = 200I_3$ and $K_v = 10000I_3$. Figures 15–17 present the results. Figure 15 shows the insertion (coordinate s_{r1} and error Δs_{r1}). Figure 16 presents the deformation (deflections *v* and *w* and the angular deviation s_{r3}). Figure 17 shows the contact forces (F_v and F_w) and the total friction force (F_{fr}). From Figure 15 we can see that the insertion error (Δs_{r1}) exponentially disappears as a result of the dynamic position control application. Hybrid control (Fig. 12) gives much greater insertion error. Better performance of the system when dynamic position control is used can be seen also comparing the diagrams of the contact force (Figs. 14 and 17) and deformations (Figs. 13 and 16).

6. CONCLUSION

In this work the general model of contact dynamics was considered. The purpose of this research is to settle all relevant dynamic effects and to derive appropriate mathematical models of contact dynamics. As the most simple representation of the "geometrical" environment was discussed first. Then, the friction between bodies in contact has been introduced. Finally, the contact of robot with dynamic environment including nonlinear effects and non-holonomic constraints has been completed. Dynamic environment was modeled by equivalent mass, stiffness and damping. The model synthesized in this manner has been applied to the

https://doi.org/10.1017/S0263574700003064 Published online by Cambridge University Press

assembling contact task. The case of robot contact with "geometrical" environment and hybrid control law have been simulated first. Then, as an environment model, more favorable dynamic environment has been considered. In that case the oscillations in contact force response and in the position of the manipulator tip have appeared, jeopardizing robot performances and in certain cases, causing the system instability. Finally, the dynamic position control and dynamic environment interacting with robot have been applied and the simulation results are compared with the previous case. Exponential decreasing of insertion error of robot tip as well as, of contact force, has pointed at the unambiguous advantage of the dynamic control with respect to the hybrid control.

References

1. M. Vukobratovic & V. Potkonjak, *Applied Dynamics and CAD of Manipulation Robots* (Springer-Verlag, 1985).
2. V. Potkonjak & M. Vukobratovic, "Dynamics of Manipulation Mechanisms with Constrained Gripper Motion – Part. 1", *Journal of Robotic Systems* **3**(3), 321–334 (1986), and M. Vukobratovic, V. Potkonjak, "Constrained Gripper Motion in Assembly Manipulation - PART 2", *Journal of Robotic Systems*, **3**(3), 335–347 (1986).
3. H. Krishnan & N.H. McClamroch, "A New Approach to Position and Contact Force Regulation in Constrained Robot Systems", *Proc. IEEE Intl. Conf. on Robotics and Automation*, Cincinnati, Ohio (1990) pp. 1344–1349.
4. S. Ahmad, "Constrained Motion (Force/Position) Control of Flexible Joint Robots", *Proc. IEEE Conf. on Decision and Control*, Brighton, England (1991) pp. 1397–1402.
5. J.K. Mills, "Stability and Control of Elastic-Joint Robotic Manipulators During Constrained Motion Tasks", *IEEE. Trans. on Robotics and Automation* **8**, No. 1, 119–125 (1992).
6. B. Brogliato & R. Lozano-Leal, "Adaptive Force/Position Control of Constrained Manipulators with Flexible Joints", *Proc. of American Control Conference*, Boston (1992) pp. 968–969.
7. M. Vukobratovic, V. Matijevic & V. Potkonjak, "Control of Robots with Elastic Joints Interacting with Dynamic Environment", *Journal of Intelligent and Robotic Systems* **23**, No. 1, 87–100 (1998).
8. M.H. Raibert & J.J. Craig, "Hybrid Position/Force Control of Manipulators", *Journal of Dynamic Systems, Measurements and Control* **103**, 126–133 [1981].
9. M.T. Mason, "Compliance and Force Control for Computer Controlled Manipulators", *IEEE Trans. on Systems, Man and Cybernetics* **11**, No. 6, 418–432 (1981).
10. T. Yoshikava, T. Sugie & M. Tanaka, "Dynamic Hybrid Position/Force Control of Robot Manipulators – Controller Design and Experiment", *IEEE Journal of Robotics and Automation* **4**, No. 6, 699–705 (1998).
11. A. DeLuca & C. Manes, "Hybrid Force/Position Control for Robots in Contact with Dynamic Environments", *Proc. of Robot Control, SYROCO '91*, Vienna (1991) pp. 377–382.
13. N. Hogan, "Impedance Control: An Approach to Manipulation", Part I–Part III, Journal of Dynamic Systems, *Measurements and Control* **107**, 1–24 (1985).
13. H. Kazeroni, T.B. Sheridan & P.K. Houpt, "Robust Compliant Motion for Manipulators, Part 1: The Fundamental Concepts of Compliant Motion, *IEEE Journal of Robotics and Automation* **RA2**, No. 2, 83–92 (1986).
14. M. Vukobratovic & Y. Ekalo, "Unified Approach to Control Law Synthesis for Robotic Manipulators in Contact with Dynamic Environment", in tutorial S5: Force and Contact Control in Robotic Systems, *IEEE Int. Conf. on Robotics and Automation* (1993) pp. 213–229; also published in *Robotica* **14**, 31–39 (1996), under title: "New Approach to Control of Robotic Manipulators Interacting with Dynamic Environment".
15. M. Vukobratovic & Y. Ekalo, "New Approach to Control of Robotic Manipulators Interacting with Dynamic Environment", *Robotica* **14**, Part 1, 31–39 (1996).
16. M. Vukobratovic, R. Stojic & Y. Ekalo, "Contribution to the Problem Solution of Position/Force Control of Manipulation Robots in Contact with Dynamic Environment – A Generalization", *IFAC Automatica* **34**, No. 10, pp. ??, 1998.

APPENDIX: POSITION/FORCE CONTROL OF ROBOTS

For better understanding of simulation experiments of position/force control in this Appendix a very concise description of conventional hybrid position/force control, as well as, a dynamic concept of position/force control of robots interacting with dynamic environment will be presented.[8–10]

Hybrid position force control. The control consists of two parallel feedback loops, the upper one for the position, and the lower one for the force. The positional loop utilizes the information obtained for the positional sensors at the robot joints, and the force loop is based on force sensing data (Fig A.1). Separate control laws are adopted for each loop. The central idea of this hybrid control method is to apply two independent control loops assigned to each DOF in the task frame. It would mean that the position control part does not interfere with the force control loop. However, that is not the actual case. Since each robot joint contributes to the control of both position and force, couplings in the manipulator mechanical structure (implied in the Jacobian matrix) cause that a control input to the actuator corresponding to the force loop (e.g. force controlled directions) produces additional forces in position controlled directions in the task frame, and vice versa. Due to this coupling between the position and force controlled DOF by setting the position errors in the force controlled directions to zero, the position feedback gains in all directions are actually reduced, causing the entire system to become more sensitive to perturbations. As a consequence, the performance of a robot is not unique with this scheme for all configurations for which, depending on selected force and position directions, the system becomes unstable.

In the force controlled directions the position errors are put to zero by a multiplication with the selection matrix orthogonal complement (position selection matrix) defined as $\bar{S} = I - S$*. Assuming a proportional plus differential position control law, and that the force control consists of a proportional plus integral controller (PI) with gain K_{Fp} and K_{Fi} respectively, as well a force feedforward part, the control law according to the scheme in Fig. A.1 can be written in the Cartesian space as:

$$\tau = K_p \bar{S} \Delta x + K_V \bar{S} \Delta \dot{x} + K_{Fp} S \Delta F + K_{Fi} S \int \Delta F \, dt + F_0 \qquad \text{(A.1)}$$

* Note that for sake of simplicity it is assumed that the task-frame coincides with the Cartesian frame. Generally the selection matrix S is not diagonal in Cartesian space.

https://doi.org/10.1017/S0263574700003064 Published online by Cambridge University Press

Based on relationships between Cartesian and joint space gains an equivalent hybrid control law in the joint space can be given in the form:

$$\tau_q = J^T \tau = K_p J^{-1} \bar{S} J \Delta q + K_V J^{-1} \bar{S} J \Delta \dot{q} + J^T (K_{Fp} S \Delta F + K_{Fi} S \int \Delta F \, dt + F_0) \qquad \text{(A.2)}$$

In order to extend the hybrid strategy to cases when the environment also exhibits a dynamic behavior, DeLuca and Manes introduces in [11] a suitable modeling of the robot-environment interaction.

Dynamic control of robotic manipulators interacting with dynamic environment. Dynamic model of the robotic mechanism interacting with the environment is described by the vector differential equation in the form:

$$H(q)\ddot{q} + h(q, \dot{q}) = \tau + J^T(q)F \qquad \text{(A.3)}$$

where $q = q(t)$ is an n-dimensional vector of robot generalized coordinates; $H(q)$ is an $n \times n$ positive definite matrix of inertia moments of the manipulation mechanism; $h(q,q)$ is an n-dimensional nonlinear function of centrifugal, Coriolis and gravitational moments; $\tau = \tau(t)$ is an n-dimensional vector of input control; $J(q)$ is an $n \times m$ Jacobian matrix relating joint space velocity to task space velocity; $F = F(t)$ is an m-dimensional vector of generalized forces or of generalized forces and moments acting on the end-effector. We adopt $n = m$ (in general $n \geq m$).

In the case when the environment does not possess the displacements (degrees of freedom) that are independent from the robot motion, the mathematical model of the environment dynamics in the frame of robot coordinates can be described by nonlinear differential equations:

$$M(q)\ddot{q} + L(q, \dot{q}) = -S^T(q)F \qquad \text{(A.4)}$$

where $M(q)$ is a non-singular $n \times n$ matrix; $L(q, \dot{q})$ is a nonlinear n-dimensional vector function; $S^T(q)$ is an $n \times n$ matrix with rank equal to n, i.e. rank $(S) = n$. Then, the system (A.3, A.4) describes the dynamics of robot interacting with dynamic environment. Here, we have to emphasize that it is assumed that the robot is permanently in contact with the environment, i.e. the robot is permanently pushing it.

The programmed motion $(PM(q_p)t)$ and desired programmed interaction force $(PFI)F_p(t)$ cannot be arbitrary. These two functions must satisfy the following relation:

$$F_p(t) \equiv f(q_p(t), \dot{q}_p(t), \ddot{q}_p(t)) \qquad \text{(A.5)}$$

The control goal of robot interacting with dynamic environment can be formulated in the following way. Let us define the control $\tau(t)$ for $t \geq t_0$, to satisfy the target conditions:

$$q(t) \to q_p(t) \text{ as } t \to \infty, \quad F(t) \to F_p(t) \text{ as } t \to \infty. \qquad \text{(A.6)}$$

Let us formulate two alternative questions.

Can we choose such a control law which, by satisfying the preset robot motion quality, would enable the attainment of the control goals that satisfy the relation (A.6)?

It is possible to choose the control law in such a way as to ensure the preset quality of the robot interaction force, and also the attainment of the control goals?

The answer to the first question is quite simple; inverse dynamics method ensures that desired motion quality is achieved and at the same time guarantees that the interaction force is stable.

Let us synthesize the control law $\tau(t)$ in such a way as to ensure a desired quality of robot motion:

$$\ddot{\eta}(t) = P(\eta, \dot{\eta}), \; \eta(t) = q(t) - q_p(t), \qquad \text{(A.7)}$$

where P is an n-dimensional vector function, such that eqn. (A.7) has unique trivial solution $\eta(t) \equiv 0$. Then the fulfilment of the requirements which have been imposed on the transient responses is ensured by the choice of the function P, and we shall design the robot control in such a way that in the absence of any perturbations except the initial ones, the robot dynamics equation coincides with eqn. (A.7). We shall *a priori* adopt that the choice of function P in the system (A.7) ensures asymptotic stability in the whole of the trivial solution of system (A.7).

Let us synthesize the control law $\tau(t)$ in such a way as to ensure a desired quality of robot motion (A.7). This can be achieved by the adopted control law having the feedback loops with respect to q, $\dot{q}$ and F:

$$\tau = H(q)\left[\ddot{q}_p + P(\eta, \dot{\eta})\right] + h(q, \dot{q}) + J^T(q)F \qquad \text{(A.8)}$$

By substituting (A.8) into the robot dynamics model (A.3), we obtain the equation of a closed-form system:

$$H(q)\left[\ddot{q} - \ddot{q}_p - P(\eta, \dot{\eta})\right] = 0 \qquad \text{(A.9)}$$

Because H(q) is a positive definite matrix, det $H \neq 0$, and, consequently, (A.9) is equivalent to (A.7). Due to the property of the function P which ensures asymptotic stability of the system (A.7) as a whole with respect to (η, $\dot{\eta}$), we will have:

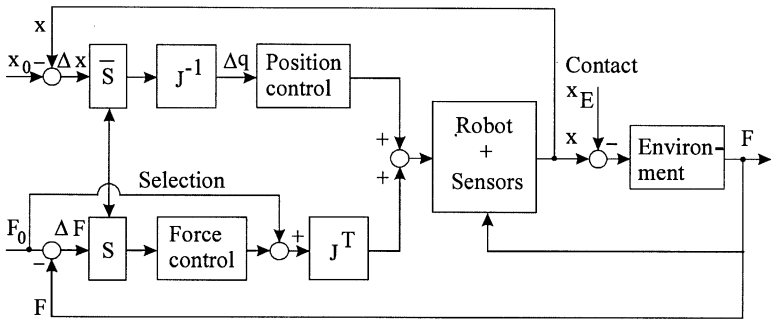


Fig. A.1. Explicit hybrid position/force control.

https://doi.org/10.1017/S0263574700003064 Published online by Cambridge University Press

$$\eta(t)_{t\to\infty}\to 0 \text{ and } \dot{\eta}(t)_{t\to\infty}\to 0 \tag{A.10}$$

and, since P is a continuous function and $P(0, 0)=0$, it follows:

$$\ddot{\eta}(t)_{t\to\infty}\to 0 \tag{A.11}$$

By comparing (A.5): $F_p(t)\equiv f(q_P(t),\ \dot{q}_P(t),\ \ddot{q}_P(t))$ and $F=f(q, \dot{q}, \ddot{q})$, we obtain the following relation between the real and programmed force of interaction, irrespective of the control law:

$$F-F_P=f(q, \dot{q}, \ddot{q})-f(q_P, \dot{q}_P, \ddot{q}_P) \tag{A.12}$$

or, by taking into account (A.7):

$$\mu=f(\eta+q_P,\ \dot{\eta}+\dot{q}_P, \ddot{q}_P+P(\eta, \dot{\eta}))-f(q_P, \dot{q}_P, \ddot{q}_P) \tag{A.13}$$

where $\mu=F-F_P$.

By taking into account the relations (A.12) or (A.13) and (A.10), (A.11), and also the continuity of the function f, we obtain:

$$\mu(t)_{t\to\infty}\to 0 \tag{A.14}$$

Thus, the control goal is achieved, i.e. along with the closeness of the real and programmed robot motion, the closeness of the real $F(t)$ and programmed $F_P(t)$ force of the interaction between the robot and the environment is attained.

However, we are now requiring something more from the force tracking: we wish to set the quality of the transient response, and we are looking for the appropriate control law.

The task of stabilizing the $F_P(t)$ can be posed in an analogous way, by considering a family of transient responses with respect to force, in the form:

$$\dot{\mu}(t)=Q(\mu),\quad \mu(t)=F(t)-F_P(t) \tag{A.15}$$

or in an equivalent form:

$$\mu(t)=\mu_0+\int_{t_0}^{t} Q(\mu(\omega))\,d\omega \tag{A.16}$$

and by choosing a continuous vector function Q(Q(0) = 0) of dimension n, such that the asymptotic stability as a whole is ensured for the trivial solution of $\mu(t)\equiv 0$.

Let us consider only one of the possible control laws with feedback loops with respect to q, $\dot{q}$ and F, of the form:

$$\tau=H(q)M^{-1}(q)\left[-L(q,\dot{q})+S^T(q)(F_P+\int_{t_0}^{t} Q(\mu(\omega))d\omega)\right] + h(q, \dot{q})+J^T(q)F \tag{A.17}$$

By applying this control law to the robot dynamics model (A.3) we obtain the following law of robot operating in contact with the environment:

$$M(q)\ddot{q}+L(q, \dot{q})=S^T(q)(F_P+\int_{t_0}^{t} Q(\mu(\omega))d\omega)$$

Taking into account the environment dynamics model (A.4), we obtain the following closed-form control system:

$$S^T(q)(\mu(t)-\int_{t_0}^{t} Q(\mu(\omega))d\omega)=0$$

and, because rank $(S)=n$, this equation is equivalent to the equation:

$$\mu(t)=\int_{t_0}^{t} Q(\mu(\omega))d\omega \tag{A.18}$$

from where, equation (A.15) follows directly.

In this way, the control law (A.17) ensures desired quality of stabilization of $F_P(t)$.

https://doi.org/10.1017/S0263574700003064 Published online by Cambridge University Press